Research Article Vol. 56, No. 32 / November 10 2017 / Applied Optics 8941

applied optics

Speckle pattern sequential extraction metric for estimating the focus spot size on a remote diffuse target

Zhan Yu,[1,2,*] Yuanyang Li,[1] Lisheng Liu,[1] Jin Guo,[1] Tingfeng Wang,[1,2] and Guoqing Yang[1,2]

[1]State Key Laboratory of Laser Interaction with Matter, Changchun Institute of Optics, Fine Mechanics and Physics, Chinese Academy of Sciences, Changchun, Jilin 130033, China
[2]University of Chinese Academy of Sciences, Beijing 100039, China
*Corresponding author: 691449010@qq.com

Received 20 July 2017; revised 3 October 2017; accepted 3 October 2017; posted 5 October 2017 (Doc. ID 302778); published 7 November 2017

The speckle pattern (line by line) sequential extraction (SPSE) metric is proposed by the one-dimensional speckle intensity level crossing theory. Through the sequential extraction of received speckle information, the speckle metrics for estimating the variation of focusing spot size on a remote diffuse target are obtained. Based on the simulation, we will give some discussions about the SPSE metric range of application under the theoretical conditions, and the aperture size will affect the metric performance of the observation system. The results of the analyses are verified by the experiment. This method is applied to the detection of relative static target (speckled jitter frequency is less than the CCD sampling frequency). The SPSE metric can determine the variation of the focusing spot size over a long distance, moreover, the metric will estimate the spot size under some conditions. Therefore, the monitoring and the feedback of far-field spot will be implemented laser focusing system applications and help the system to optimize the focusing performance.

OCIS codes: (030.6140) Speckle; (120.6150) Speckle imaging; (140.3295) Laser beam characterization; (140.3490) Lasers, distributed-feedback.

https://doi.org/10.1364/AO.56.008941

1. INTRODUCTION

In some applications, it is necessary to acquire a focusing spot with high energy density when the laser beam concentrates on a remote target. Some factors will appear in the process of the laser beam propagation, which influence the concentration effect of far-field beam energy, for example, the system jitter, the atmospheric turbulence, and the system aberration. In order to obtain a high energy density focusing spot in the remote laser focusing system, it is necessary to have an observation system to supervise the focal spot so that the spot information can be fed back to the focusing system, which will improve the system focusing effect.

When a diffuse target is illuminated with a laser beam, the reflected field will generate a grain-like distribution due to the interference of the fields reflected from different parts of the rough target surface. The diffuse light field in this situation is called the speckle field. The method to supervise the remote laser spot is based on the reflected speckle, which has been applied [1] to the laser projection system because the speckle field will carry the information about the beam parameters of the rough surface. This information can be extracted by speckle interferometry [2], speckle photography [3], and many other methods [4,5]. If the roughness of the diffuse target surface is relatively large [the root mean square (RMS) roughness is larger than the wavelength], the target surface property does not affect the second-order statistical property [6–8] of the reflected speckle field. In this situation, the speckle field scattered by the rough surface is generally called a fully developed one. Based on Goodman's theory [9], the average speckle size of the fully developed speckle field is inversely proportional to the beam spot size on the rough surface. Hence, the statistics property of the speckle field can provide metrics for estimating the laser beam that concentrates on the remote rough target surface.

By studying the wavefront detection theory [10–13], the laser beam that focuses on the remotely located target can be achieved, and this result is verified by experiments [14]. But, the phase modulation caused by the light field that illuminates on the rough surface of the target is difficult to correct by the brightness function, it impacts on the focus performance of the far-field beam energy. Vorontsov and many other scientists introduce some methods [15,16] to improve laser beam concentration on extended objects, which is based on optimization of the speckle-field-based metric by the stochastic parallel gradient descent (SPGD) technique. If we do not use the method

of wavefront detection to optimize the focusing spot on the remote target, the optimization algorithm can replace it, such as the SPGD technique. The final optimized result by means of the SPGD algorithm is determined by the beam quality metric performance. By analyzing the statistical properties of speckle, some reliable beam quality metrics can be obtained, for example, the changes of power in the bucket (PIB) variance [17] of reflected speckle, the clipped speckle autocorrelation (CSA) [18] metric, and the clipped speckle edge integration (CSEI) [10] metric; their feasibility is verified by experiments.

The PIB, CSA, and CSEI metrics can reflect the variation trend of the focusing spot size, but the theoretical restrictions of application are not given, and they did not make further analysis of the theoretical results of the metrics. In this paper, we propose a new metric to solve the above problem, which is the speckle pattern sequential extraction (SPSE) metric. The SPSE metric is for estimating the focusing spot size on the remote diffuse target, where this beam quality metric is based on the statistical characteristics of speckle field intensity distribution. This method is applied in the target-in-the-loop beam control system, which can reflect the variation trend of the focusing spot size and improve the effect of focusing on the remote rough target surface. The actual output of metric combined with the theoretical value can estimate the immediate size of the focal spot, and the metric limitation can be obtained by theoretical derivation. Due to the acquisition process of the SPSE metric being simple, the calculation is faster.

2. THEORY OF SPECKLE INTENSITY LEVEL CROSSING

The statistical properties of the speckle field intensity distribution when received by the observation system can give a metric to achieve the estimation of the beam spot size on the remote diffuse target. It follows the theory, in which the fully developed speckle field spatial correlation radius (speckle size) a_s at the receiver plane is inversely proportional to the beam spot size b on the rough surface: $a_s = \lambda L/b$, where L is the length of propagation path, and λ is wavelength. Therefore, based on this theory, speckle size at the receiver plane can be used as a laser beam quality metric (speckle metric) J_s to estimate the focus spot size on the diffuse target.

According to the theory, the speckle size is inversely proportional to the beam spot size on the rough surface; if the aperture size of the observation system is given, the number of speckles in the receiving pattern will reflect the focusing spot size on the far-field diffuse target. Therefore, in this paper, the speckle intensity level crossing model is used to obtain speckle information. The one-dimensional speckle intensity level crossing model is shown in Fig. 1. A specific I_1 as the intensity threshold to the pattern of a one-dimensional speckle intensity distribution was set, and the expected value of speckle intensity across threshold is expressed as $E[N_s]$. According to the statistical theory of speckle, there exists a statistical correlation between $E[N_s]$ and the size of speckle. In this paper, we use a method of Rice [19] to obtain the expected number of crossings about the intensity level in the speckle pattern. In the pattern of Gaussian speckle field, the expected number of crossings about level I_1 in the interval (x_1, x_2) is given by

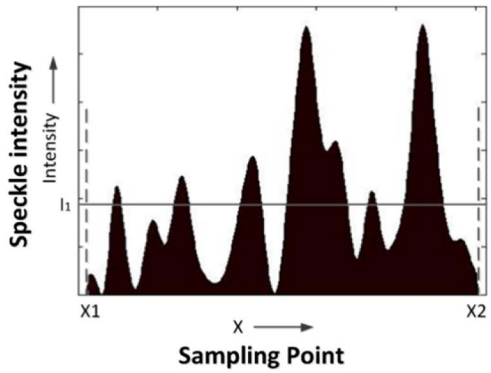

Fig. 1. Crossings about intensity level I_1 in a normal speckle pattern.

$$E[N_s] = \int_{x_1}^{x_2} \mathrm{d}x \int_{-\infty}^{\infty} |\eta| P(I_1, \eta) \mathrm{d}\eta, \tag{1}$$

where $P(I_1, \eta)$ is the joint density of I_1 and η, η is the derivative of speckle intensity. The first-order probability density of speckle intensity is a negative exponential. Therefore, the second-order joint probability density $P(I_1, I_2)$ is given by [5]

$$P(I_1, I_2) = \frac{\exp\{-(I_1 + I_2)/\langle I\rangle[1 - |\mu_A(\Delta x)^2|]\}}{\langle I\rangle^2[1 - |\mu_A(\Delta x)^2|]} \times I_0\left(\frac{2\sqrt{I_1 I_2}|\mu_A(\Delta x)|}{\langle I\rangle[1 - |\mu_A(\Delta x)^2|]}\right), \tag{2}$$

where I_0 is the modified Bessel function of the first kind, $\langle I\rangle$ is the average intensity of the speckle field, I_1 and I_2 are the intensities at the two points, $\mu_A(\Delta x)$ is the amplitude correlation coefficient for the two points, and $0 < |\mu_A(\Delta x)| < 1$. In Eq. (1), η is the slope given by

$$\eta = \lim_{\Delta x \to 0}(I_2 - I_1)/\Delta x. \tag{3}$$

Taking Eq. (3) into Eq. (2), the $P(I_1, \eta)$ can be given as

$$P(I_1, \eta) = \frac{\exp(-I_1/\langle I\rangle)}{2\sqrt{\pi}\langle I\rangle^{3/2} I_1^{1/2}} \lim_{\Delta x \to 0} \frac{\Delta x}{[1 - |\mu_A(\Delta x)|^2]^{1/2}} \times \exp\left(\frac{\eta^2 (\Delta x)^2}{4 I_1 \langle I\rangle[1 - |\mu_A(\Delta x)|^2]}\right). \tag{4}$$

Expand the $\mu_A(\Delta_x)$ into the Taylor series, and, based on the derivative definition, Eq. (4) can be turned into

$$P(I_1, \eta) = \frac{\exp(-I_1/\langle I\rangle)}{2\sqrt{\pi} I_1^{1/2}\langle I\rangle^{3/2}} \times \frac{1}{[-|\mu_A(0)|'']^{1/2}} \times \exp\left(\frac{-\eta^2}{4 I_1 \langle I\rangle[-|\mu_A(0)|'']}\right). \tag{5}$$

Substituting Eq. (5) into Eq. (1), the expected number of crossings about level I_1 in the interval (x_1, x_2) is given by

$$E[N_s] = \frac{2}{\sqrt{\pi}}[-I_1|\mu_A(0)|''/\langle I\rangle]^{1/2} \exp\left(-\frac{I_1}{\langle I\rangle}\right)(x_2 - x_1). \tag{6}$$

From this expression, we can find that the expectation is mainly determined by the function $|\mu_A(\Delta x)|''$; this function describes the cross-correlation value of the two points on

the receiving plane. If the light spot on the diffuse target surface is a square scattering spot, the size is L. The distance from the target to the observation system is Z. We have

$$\mu_A(\Delta x) = \mathrm{sinc}\left(\frac{L\Delta x}{\lambda Z}\right) / \frac{\pi L \Delta x}{\lambda Z}, \tag{7}$$

whereby

$$|\mu_A(0)|'' = -\frac{1}{3}\left(\frac{\pi L}{\lambda Z}\right)^2. \tag{8}$$

Taking Eq. (8) into Eq. (6), we can obtain

$$E[N_s] = 2\left(\frac{\pi}{3}\right)^{1/2}\left(\frac{I_1}{\langle I\rangle}\right)^{1/2} \exp\left(-\frac{I_1}{\langle I\rangle}\right)\frac{x_2 - x_1}{\lambda Z/L}. \tag{9}$$

In Eq. (9), we can find that $E[N_s]$ is in direct proportion to the beam spot size L on the rough surface. That is to say, if the intensity threshold I_1 and the receiving distance Z are definite, when the size of beam spots on the rough surface increases, the expected value of crossings about the intensity threshold in the speckle intensity distribution pattern will increase correspondingly. We can use this character to estimate the focus spot size on the remote diffuse target.

3. SPECKLE PATTERN SEQUENTIAL EXTRACTION METRIC

In the case that applies speckle field to estimate the far-field spot size, after taking the sequential extraction of the collected three-dimensional speckle field, the multiple sets of one-dimensional speckle intensity distribution patterns are obtained. By analyzing these patterns, a beam quality metric can be obtained.

As Fig. 2(b) shows, in the laser focusing system, the echo signal obtained by the CCD is the speckle field that is produced by the diffuse reflection of the focusing spot illuminated on the remote rough target. As Fig. 2(a) shows, the speckle field signal is a three-dimensional pattern, which is composed of two-dimensional speckle position distribution information and speckle intensity information. The pattern is two-dimensional speckle intensity distribution information. In the fully developed speckle field, we consider that each phase is statistically independent of all of the others. Therefore, we can regard the two-dimensional speckle intensity distribution pattern as the $N*N$-dimensional matrix. We consider that the pattern of two-dimensional speckle intensity distribution is decomposed into N groups patterns of one-dimensional speckle intensity distribution, as shown in Fig. 2(c). Calculating the number of crossings about the intensity threshold in each one-dimensional speckle intensity pattern and stacking them together, the resulting J_s is the speckle metric:

$$J_s = \sum_{i=1}^{n} Ni, \tag{10}$$

where N_i is the number of crossings about the intensity level in the ith one-dimensional speckle intensity pattern (the number of intersections when intensity distribution crosses the threshold I). The selection of speckle intensity crossed threshold I selection is generally chosen to receive half of the average intensity of the speckle field obtained within the aperture of the receiving system. As shown in Eq. (9), when the speckle field within the aperture of the receiving system is determined, the selection of the intensity threshold directly affects the number of one-dimensional speckle that crosses the intensity threshold. In this paper, the number of crossings about the intensity level is applied to obtain the speckle metric. Therefore, in order to make the metric more accurate, the selected intensity threshold can be used to make the number of crossings about the threshold in the speckle pattern to reach the maximum. According to the research results of Bahuguna *et al.* [20], when the selected intensity level is half of the average intensity of the speckle field, the expected number of crossings about the intensity level is the maximum; it is about $0.87(x_2 - x_1)/(\lambda Z/L)$. Under this condition, we can get the theoretical output based on the SPSE metric.

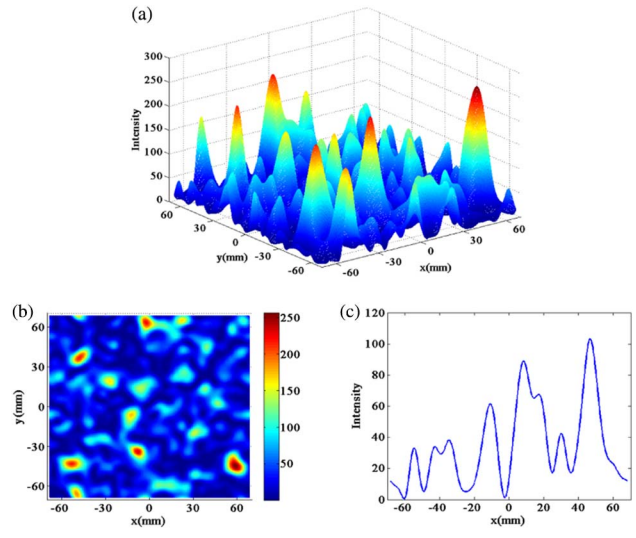

Fig. 2. Pattern of speckle intensity distribution.

A. Simulation Analysis of the SPSE Metric

This section introduces the simulation method of obtaining the SPSE metric and makes a simple analysis of the simulation results. The surveillance system of a focusing spot on a far field includes the omitting and receiving processes. Due to the transmitting propagation path of laser focusing not being related to the main problem discussed in this section, the receiving path is the only topic to discuss in the simulation process. The propagation process of a focusing spot from a diffuse target to the receiving system adopts the transmission model illustrated in Fig. 3.

In the simulation process of speckle field propagation, the one step fast Fourier transform (FFT) method is applied. In the simulation, the FFT method needs a square matrix of dimension $N \times N$ to describe the input and output fields. In this paper, we set $N = 512$, the length of the input plane is $L = 200$ mm, the sampling interval in the input plane is L/N, the wavelength is $\lambda = 0.532$ μm, and the observation system is 100 m from the diffuse target ($Z = 100$ m). In the simulation, regarding the received speckle field as a fully developed speckle field, the diffuse target model is established by random phase distributions, which are randomly generated from 0 to 2π to obtain a set of phase screens. The simulation

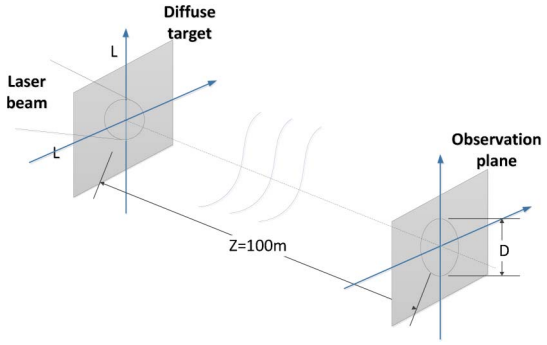

Fig. 3. Transmission model of speckle field.

process is shown in Fig. 2, and the received speckle field is decomposed into N groups of distribution patterns for one-dimensional speckle intensity. In order to improve the calculating speed, each group of patterns has been binarized. If it is greater than the threshold, then mark it as one, if it is less than the threshold, mark it as zero. In each of the obtained arrays, if the value of the adjacent elements changes once, the intensity is considered to cross the threshold once. The total number of changes in the array is regarded as the number of the speckle intensity crossing the threshold, and the sum value of the N groups is the value of the speckle metric.

Figure 4 is the theoretical results of the SPSE metric. The focusing spot size varies from 0.6 to 6.5 mm, and the variation interval is 0.1 mm. It can be seen from Fig. 4 that the output value of the speckle metric increases when the focus spot size increases, and the SPSE metric and the focusing spot size show a linear relationship. In practice, when the output value of the speckle metric and focusing spot size changes are in a similar linear relationship, we consider that the metric can estimate the changes of the focusing spot size, and the metric is effective at the moment.

Figure 5(a) shows the SPSE metric simulation results, the selection of related parameters in the simulation process is the same with the corresponding parameter in Fig. 4. Due to the random error generated by the difference between the sample and the population in the process of random sampling,

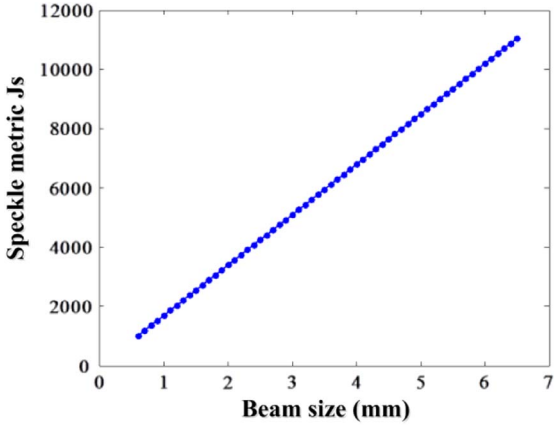

Fig. 4. Theoretical output of the speckle pattern sequential extraction metric.

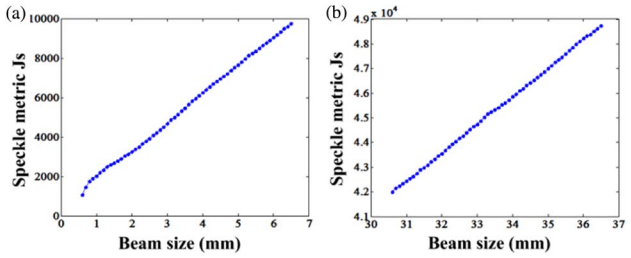

Fig. 5. Simulation results of speckle metric. (a) The focus spot size varies from 0.6 to 6.5 mm. (b) The focus spot size varies from 30.6 to 36.5 mm.

there is a deviation from the theoretical output, but the SPSE metric and the focusing spot size show a linear relationship. With the increasing of the focusing spot size, the output of the speckle metric increases, the simulation output and the theoretical output change in the same trend, and the feasibility of the SPSE metric is proved. From the simulation results in Fig. 5(a), it can be concluded that the speckle metric can effectively reflect the variation of focusing spot size when the spot size varies from 0.6 to 6.5 mm.

In the same simulation conditions, enlarging the focal spot size to make the variation range from 30.6 to 36.5 mm, the simulation result is shown in Fig. 5(b). It can be seen that when the size of the focal spot increases, the speckle size will decrease, and as the number of speckle in the received pattern increases, the metric output is obviously improved. From the simulation results in Fig. 5(b), we will find that the metric keeps a linear relationship with the focal spot size, and this relationship is consistent with the theoretical analysis. It can be considered that the SPSE metric can estimate the change of the focal spot size. In the simulation, we found that although the enlarging number of speckle leads to an increase of calculated amount, there is almost no change on the speed of the obtained metric when the change interval of the focus spot size varies from 0.6–6.5 mm to 30.6–36.5 mm through the method of timing measurement. In the actual situation, when the receiving system is 100 m from the target, and the focal spot size on the target surface reaches 30 mm, the method of telescope system direct imaging can be used to estimate the variation of spot size. Therefore, in the simulation of the SPSE metric, there is no need to continue to expand the spot size for further discussion; when the focusing spot is large, the metric can effectively estimate the spot size.

B. Two Theoretical Limitations of Speckle Metric

In this section, the state of the SPSE metric when the focusing spot size is in its maximum and minimum through the method of theoretical analysis that combined with simulation will be analyzed, and the theoretical scope of the speckle metric will be given. The selected parameters involved in the simulation are the same as with previous ones.

As shown in Fig. 6(a), when the focusing spot size is very small, the metric cannot estimate the variation of the spot size. Due to the speckle size being larger when the focusing spot size becomes smaller, and there are fewer speckles in the aperture of the observation system, it causes an insufficient number of

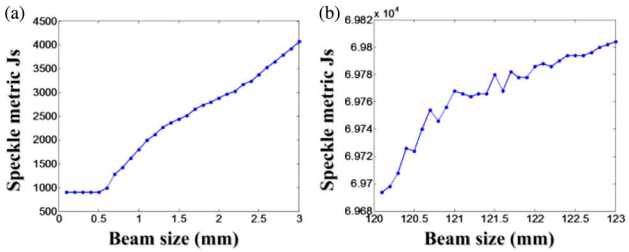

Fig. 6. Metric simulation results in which the focusing spot size is in its maximum and minimum. The graphs (a) and (b) abscissa is the focusing spot size, the ordinate is the metric output. In graph (a), the spot size ranges from 0.1 to 3.0 mm, and, in graph (b), spot size ranges from 120.1 to 123.0 mm.

speckle samples and increases the measurement errors. When the spot size reduces to a critical value (the expected number of crossing about the level is less than two), the number of speckle intensity crossings of the threshold does not change with the spot size, and the speckle metric will lose efficacy in this time.

As shown in Fig. 6(b), when the focusing spot size is very large, the speckle metric cannot estimate the variation of spot size. This phenomenon is due to the focusing spot size being larger, the speckle size is smaller, and there are more speckles in the aperture of the observation system; when the resolution of observation system is definite, the expected number of crossings about the intensity threshold is greater than one-half the actual number of sampling points, so we cannot completely distinguish the speckles in the receiving plane. It will affect the value of metric output, and the speckle metric will lose efficacy in this time.

According to the above analyses, the applicable range of the speckle metric can be obtained from the simulation based on these observation system parameters, which turned out to be from 0.6 to 120.4 mm.

C. Influence of the Aperture of the Observation System

When the focusing spot is smaller, the echo speckle size is larger, and there are fewer speckles in the receiving plane. If the aperture of the observation system has a small size, it will cause the number of speckle samples to be insufficient, and it increases the measurement errors. Therefore, the aperture of the observation system has an important impact on the speckle metric.

In this paper, we propose the method to count the number of the speckle intensity crosses of the threshold, which will reflect the number of speckles in a region of the received speckle pattern so as to estimate the size of the focal spot. Therefore, in order to ensure the effectiveness of the speckle metric, it is necessary to have at least one of the one-dimensional speckle patterns after the receiving speckle pattern is extracted; the number of speckle intensity distributions crossing the intensity threshold is greater than two under the theoretical limits. That is the expected number of crossings about the intensity threshold, which is larger than 2 ($E[N_s] > 2$). When the selected intensity threshold is a half of the average intensity of the speckle field, according to Bahuguna's conclusion, we can obtain

$$L > \frac{2\lambda Z}{0.87(x_2 - x_1)}. \tag{11}$$

From Eq. (11), when the aperture size of the observation system is definite, the minimum value of the focal spot size can be theoretically estimated by the speckle metric.

In the application, the observation system with different apertures will have an influence on the speckle metric output. Therefore, the observation system with different apertures is selected to analyze the simulation results of the SPSE metric output. Figure 7 shows the simulation results of the speckle metric, where the focusing spot size ranges from 0.15 to 1.60 mm, the observation system is 100 m from the target, and the aperture sizes of the observation system are 100 and 130 mm. There is a method of judgment on whether the speckle metric is effective in the application. When the focal spot size gets larger, the output of the speckle metric gets larger, so the metric can estimate the variation of spot size; therefore, the metric is effective at the moment. However, the metric cannot be considered effective in any other conditions. According to this principle, observing the circle marked parts in Fig. 7, it can be seen that the aperture size of the observation system is larger, so the speckle metric that can effectively estimate the minimum size of the focusing spot is smaller. By means of abundant simulation analyses, if the aperture of the observation system is definite, the minimum size of the focusing spot, which can be estimated by the speckle metric under the limited condition, is consistent with the conclusion of the Eq. (11). This conclusion can be applied to select the aperture size of the observation system:

$$D > \frac{\lambda Z}{0.87\omega}, \tag{12}$$

where ω is the minimum spot size of the focal spot, Z is the distance from observation system to the diffuse target, and λ is the wavelength.

In the application of speckle metric, the metric is required not only to provide the variation trend of the focusing spot size, but also to obtain the size estimation of the focal spot. Therefore, it is necessary to combine the actual output of metric with the theoretical output value of speckle metric to analyze the

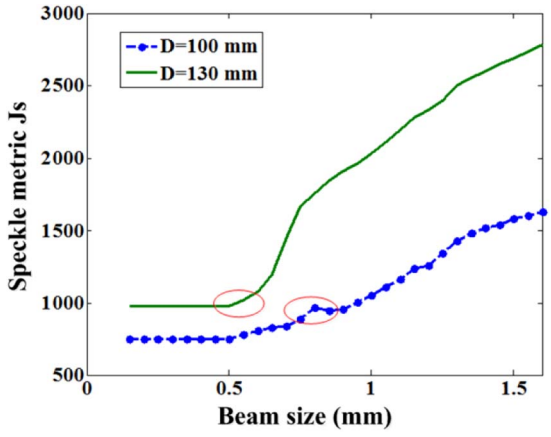

Fig. 7. Simulation results of speckle metric when aperture size of the observation system are 100 and 130 mm.

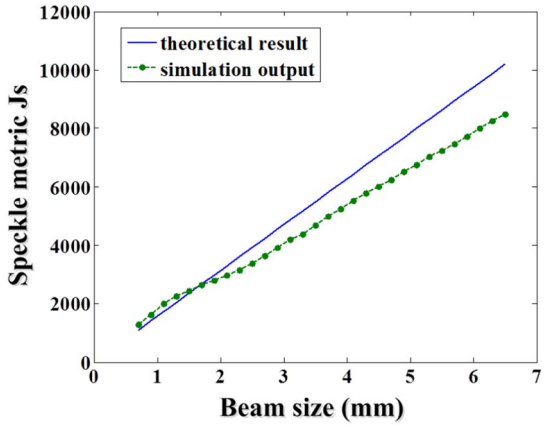

Fig. 8. Simulation results and the theoretical output of the speckle metric when the aperture size of the observation system is 120 mm.

focusing spot size. Figure 8 shows the simulation output and the theoretical output of the speckle metric when the observation is 100 m from the target, the size of focal spot ranges from 0.7 to 6.5 mm, and the aperture of the observation is 120 mm.

From the Fig. 8, when the focal spots are the same size, their theoretical value and the output results of the speckle metric have deviations. The expected number of crossings over the intensity threshold in the complete speckle field needs to be the maximum when the theoretical results of the speckle metric are calculated. Therefore, the theoretical results of the metric are related to the selected intensity threshold and the probable density of the intensity distribution in the complete speckle field. In the process of collecting the speckle pattern, there is a difference between the received speckle intensity distribution and the intensity distribution of the whole speckle field. In this situation, when we selected the same intensity threshold, the theoretical results and the simulation output of the speckle metric exist with deviations. Applying the method of multiple sampling to take the mean value can reduce the deviation between them.

In Figs. 9(a) and 9(b), the simulation output is the mean value of the speckle metric output, which is obtained by the observation system through multiple sampling and respectively calculating the metric output. The error bars indicate the deviation ranges for the corresponding simulation output of the speckle metric. In order to facilitate the calculation, we extract four sets of one-dimensional speckle intensity patterns in

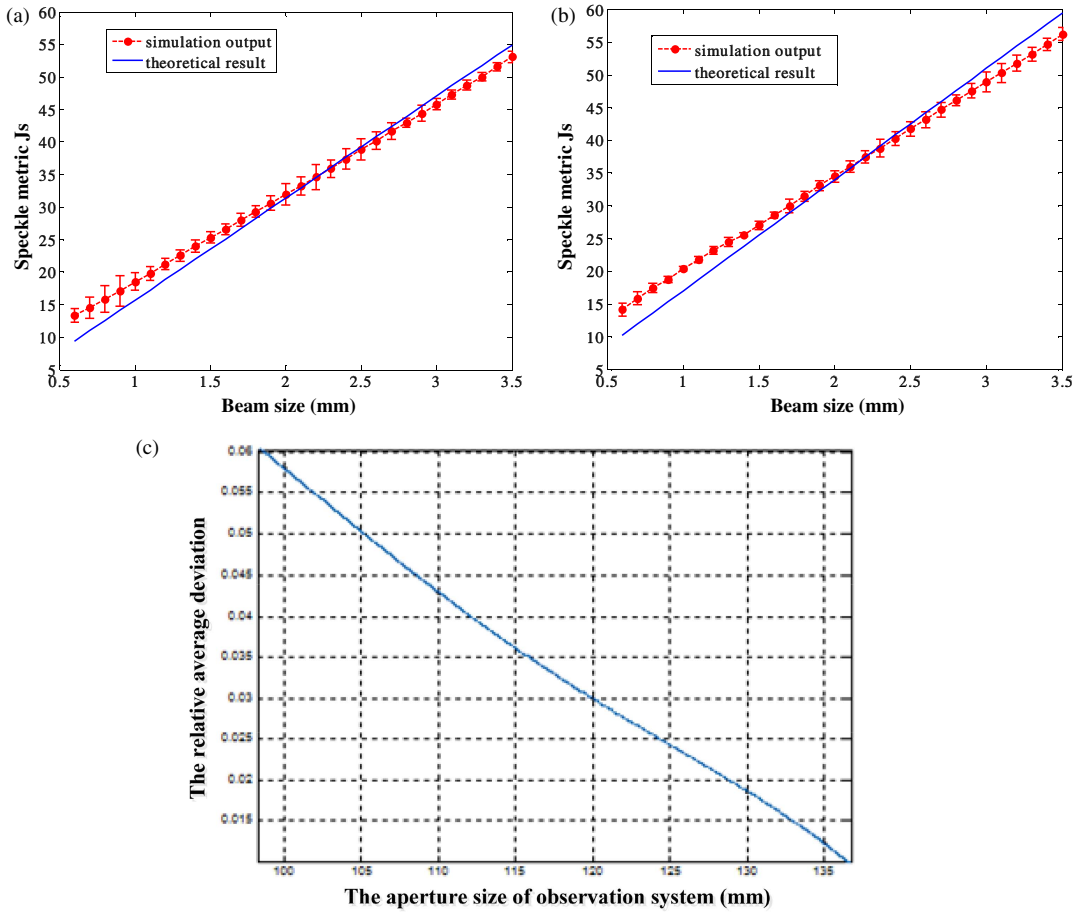

Fig. 9. Simulation analysis of SPSE metrics in different apertures of the observation system. (a) The aperture size of the observation is 120 mm. (b) The aperture size of the observation is 130 mm. The error bars are the deviation ranges for the corresponding simulation output of the speckle metric. (c) The abscissa is the aperture size of the observation system, and the ordinate is the relative average deviation between the theoretical results and the mean value of the speckle metric output when the size of the focal spots is in the same range under the observation system surveillance.

each received echo speckle field for analysis in the simulation. In the simulation process, the selection of related parameters is the same as before except the size of the focal spot, and the range is from 0.5 to 3.5 mm. Figures 9(a) and 9(b) show that when the aperture size of observation gets larger, the deviation between the mean value of the speckle metric and the theoretical value gets smaller. Figure 9(c) shows the mean variation between the theoretical results and the mean value of the speckle metric output in different observation systems. With the aperture size of the observation system getting larger, the mean variation to its theoretical value gets smaller. When the aperture size increases, the number of the speckle in the received pattern gets larger, and the measurement accuracy of the metric will improve. In the meantime, the probability density of the received speckle intensity distribution approaches the echo speckle field, and the simulation output tends to its theoretical results.

Figures 9(a) and 9(b) show the same phenomenon, in which both ends of the curve gradually deviate from the theoretical value. Due to the size of focal spot being smaller, the speckle size is larger, and there are fewer speckles in the observation system, which will affect the measurement accuracy. When the size of focal spot gets larger, there are more speckles in the observation system, and the sampling interval of observation restricts the accuracy of measurement. We can increase the value of N to solve this problem in the simulation process.

The method of multiple sampling is applied to obtain the mean value of the speckle metric output, and the mean value combined with the theoretical results will help to estimate the size of remote focusing spots. In the application of this method, the amount of computation is large, and the time for calculation is long. The method through placing multiple linear array detectors to receive speckle field information at the same time can be used to solve this problem.

4. EXPERIMENT

The experimental device for testing the feasibility of the SPSE metric is shown in Fig. 10. This experimental device is mainly composed of four parts: the laser focusing system, the observation system, the signal processing system, and the laser beam profile detection system. In the experiment, we focus a continuous wave laser whose wavelength is 0.532 μm on a diffuse target, and the observation system collects the returned speckle field, which is generated by a laser beam illuminating on the diffuse target surface. The observation system consists of a camera lens with an aperture size of 107 mm and a complementary metal–oxide–semiconductor (CMOS) camera with a pixel size of 12 μm, and the F-number of the observation system lens is 2.8. The distance from the diffuse target to the objective lens of the observation system is 5.4 m. We change the distance between the focusing lens and the diffuse target to obtain a different size of focusing spot by moving the diffuse target. Due to laser beam transmission distance being much larger than the variation, this method does not affect the results of the final analysis. In the process of image acquisition by adjusting the defocus amount, we can obtain a clearer speckle image and maintain this parameter to collect speckle information. The diffuse target we selected is not polished and marked with a no scratches metal plate in our experiments. The signal processing system converts the received speckle field into the information of speckle intensity distribution, and, after calculation, we will obtain the speckle metric output. The laser beam profile detection system will directly get the information of the focusing spot size on the target, which helps us verify the speckle metric performance. In the experiment, the selection of the speckle intensity threshold needs to be increased appropriately, due to the consideration of background noise influences in the experiment. There is another way to reduce the noise influence, which is to filter out the background light in the received speckle pattern with the signal processing, and select the intensity threshold to obtain the speckle metric output. When the metric output is obtained, the laser beam profiler is applied to replace the diffuse target for obtaining the actual size of the corresponding focal spot, so that the experimental results can be verified and analyzed. In the experiment, we use the slide way to calibrate the position of the focusing spot, where it will make the laser beam profiler remain in the same position as the spot. In order to make the conclusions of the

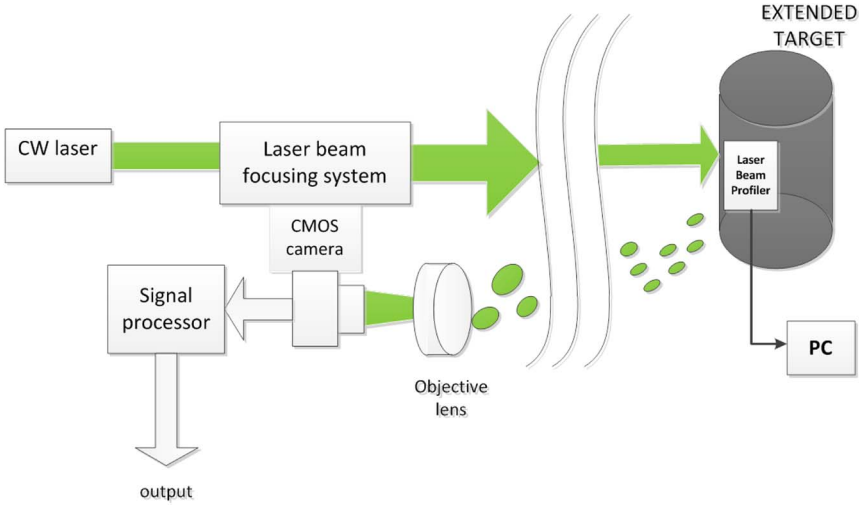

Fig. 10. Experimental device for testing the feasibility of the SPSE metric. CW, continuous wave; PC, personal computer.

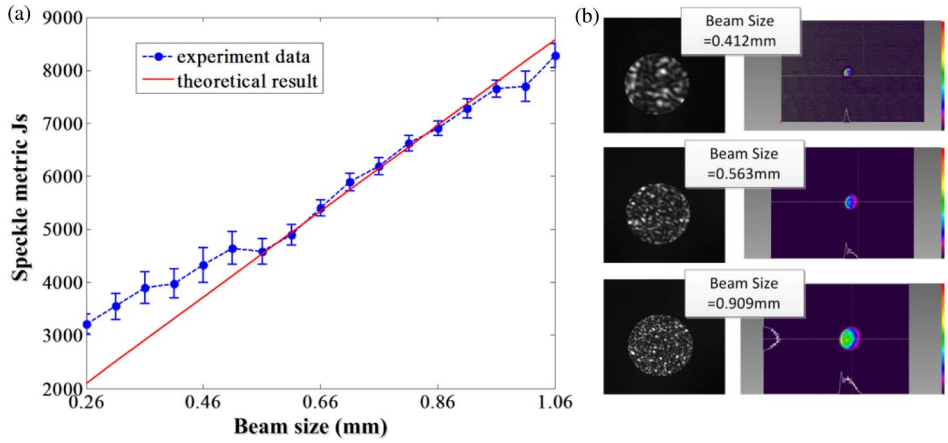

Fig. 11. (a) Experimental results of the SPSE metric. (b) Part of the speckle patterns obtained in the experiment and the corresponding focal spot images, which were obtained from the target surface. In the image plane, 12.288 mm corresponds to these speckle patterns. The beam size is obtained by a least squares Gaussian fitting of the spot.

analysis more convincing, we selected six sampled positions on the surface for a per beam size.

The experimental results of the SPSE metric are shown in Fig. 11(a), where the marker is the mean value of the six sets of experimental results of speckle metrics; the solid line is the theoretical calculation result, and the error bars indicate the deviation ranges for the corresponding experimental results of the speckle metric. It can be seen from the experimental data, when the size of focal spot gets larger, the value of the speckle metric output gets larger; they approximately keep a linear relationship, which is in accord with the above simulation analyses. At the same time, compared with the experimental results and theoretical output, it can be seen that the output curve of the speckle metric obtained by the experiment deviates from the theoretical result at both ends, and the middle part agrees with the theoretical result, which is consistent with the result obtained by a previous simulation. Therefore, the experimental results verify the conclusions of theoretical analysis and simulation analysis.

In the experiment, we use the Gaussian beam as the light source. There are aberrations caused by the laser focusing system, but, as explained below, these aberrations do not affect us estimating the variations of focusing spot size through the SPSE metric. In the experiment, the laser spot size is obtained by least squares Gaussian fitting of the spot, and the size of the beam obtained by this method can reflect the size of the focusing spot. We use the one-dimensional speckle intensity level crossing model to obtain the speckle metrics; if the focusing spot size we got by Gaussian fitting is along the X axis, the one-dimensional intensity information we extracted is necessarily distributed along the X axis. Therefore, we consider that the anisotropy of spots has little effect for the SPSE speckle metric. It can be seen from Fig. 11(a) that the experimental results are consistent with the simulation results in Fig. 9. This deviation phenomenon also appears in the simulation when we use isotropic spots. It proves that the anisotropy of the spot is not the cause of the deviation between the experimental results and the theoretical results. Therefore, we consider that there are two main reasons for which the experimental results are greater than the theoretical results when the focusing spot size is very small. First, there are fewer speckles in the aperture of the observation system, which causes the number of speckle samples to be insufficient and increases the measurement errors. Second, in the application, in order to improve the accuracy of the speckle metric, it is necessary to extract abundant information of one-dimensional speckle intensity from the received speckle pattern, and, in the process of sequentially extracting the intensity information, the sampling density is larger. As shown in Fig. 11(b), when the focusing spot size is smaller, the presence of each speckle in the received speckle pattern will affect many groups of extracted one-dimensional speckle intensity information, lead to a large correlation among the data, and enlarge the speckle metric output. But, in the process of calculating the theoretical output by crossing the intensity thresholds, each set of data, which is described by speckle intensity distribution, is independent. Therefore, the output value of the speckle metric, which is obtained by experimental data, is greater than the theoretical result. It is proved in the simulation that this error can be eliminated if the system aperture is apparently increased. As shown in Fig. 11(b), when the focusing spot size is very large, there are a mass of speckles in the observation system, and the speckle size is very small. Due to the limitations of the CMOS camera pixel size, we cannot completely distinguish all of the speckles in the patterns, which were obtained by extracting the received speckle field; therefore, the speckle metric outputs are reduced. In order to make the output of the speckle metric closer to the theoretical results, it is necessary to select smaller pixel size CMOS camera to improve the resolution precision.

5. CONCLUSION

In this paper, based on the one-dimensional speckle intensity level crossing theory, we propose a method of sequentially extracting the pattern of received echo speckle field to obtain the speckle metric. The speckle metric obtained by this method can effectively judge the changing information of focal spot size on a remote target; moreover, it will achieve the supervision and

feedback of the target spot in the laser far-field focusing application. This method helps the focusing system optimize the focusing effect and obtain a focal spot with high energy density. Combined with theoretical analyses, the feasibility of the speckle metric is verified by simulation analysis, and the applicable range of metric is given. Only when the metric meets the conditions, in which the wavelength is 0.532 μm, the target is 100 m from the observation system, the aperture of the observation system is 100 mm, and the pixel size is 0.266 mm, can it theoretically judge the changing range of focal spot size, where the range is from 0.6 to 120.4 mm in its maximum. Then, we discuss the effect of speckle metric on the aperture of observation system, and the selection rule of aperture is given according to Eq. (11). The method of multiple sampling is applied to take the mean value of the metric output so that the estimation of the far-field focal spot size can be achieved, and this method is verified by means of simulation. In this paper, the experiment results show that the output of metric is consistent with its theoretical analysis results when the focal spot changes from 0.26 to 1.06 mm. Therefore, the performance of the speckle metric is verified by experiments. The SPSE metric is applicable only when the diffuse target is in a relatively static state.

Funding. Key Research Program of Frontier Sciences, Chinese Academy of Sciences (CAS) (QYZDB-SSW-SLH014).

REFERENCES

1. T. Sawatari and A. C. Elek, "Image plane detection using laser speckle patterns," Appl. Opt. **12**, 881–883 (1973).
2. T. Yoshimura, M. Zhou, K. Yamahai, and Z. Liyan, "Optimum determination of speckle size to be used in electronic speckle pattern interferometry," Appl. Opt. **34**, 87–91 (1995).
3. S. E. Skipetrov, J. Peuser, R. Cerbino, P. Zakharov, B. Weber, and F. Scheffold, "Noise in laser speckle correlation and imaging techniques," Opt. Express **18**, 14519–14534 (2010).
4. D. V. Semenov, S. V. Miridonov, E. Nippolainen, and A. A. Kamshilin, "Statistical properties of dynamic speckles formed by a deflecting laser beam," Opt. Express **16**, 1238–1249 (2008).
5. J. C. Dainty, *Laser Speckle and Related Phenomena* (Springer, 1975).
6. J. C. Dainty, "Some statistical properties of random speckle patterns in coherent and partially coherent illumination," Opt. Acta **17**, 761–772 (1970).
7. R. Barakat and J. Blake, "Second-order statistics of speckle patterns observed through finite-size scanning apertures," J. Opt. Soc. Am. **68**, 614–622 (1978).
8. R. G. Berlasso, F. P. Quintián, M. A. Rebollo, N. G. Gaggioli, L. M. Sánchez Brea, and E. B. Martínez, "Speckle size of light scattered from slightly rough cylindrical surfaces," Appl. Opt. **41**, 2020–2027 (2002).
9. J. W. Goodman, "Some fundamental properties of speckle," J. Opt. Soc. Am. **66**, 1145–1150 (1976).
10. M. A. Vorontsov and G. W. Carhart, "Target-in-the-loop adaptive optics: wavefront control in strong speckle-modulation conditions," Proc. SPIE **4825**, 67–73 (2002).
11. C. Wang, "High-speed SPGD wavefront controller for an adaptive optics system without wavefront sensor," Proc. SPIE **7658**, 76585T (2010).
12. V. V. Dudorov, M. A. Vorontsov, and V. V. Kolosov, "Speckle-field propagation in 'frozen' turbulence: brightness function approach," J. Opt. Soc. Am. A **23**, 1924–1936 (2006).
13. M. A. Vorontsov and V. Kolosov, "Target-in-the-loop beam control: basic considerations for analysis and wave-front sensing," J. Opt. Soc. Am. A **22**, 126–141 (2005).
14. M. A. Vorontsov, V. V. Kolosov, and E. Polnau, "Target-in-the-loop wavefront sensing and control with a Collett-Wolf beacon: speckle-average phase conjugation," Appl. Opt. **48**, A13–A29 (2009).
15. M. A. Vorontsov and G. W. Carhart, "Adaptive phase distortion correction in strong speckle-modulation conditions," Opt. Lett. **27**, 2155–2157 (2002).
16. M. Voronstov, J. Riker, E. Polnau, S. Lachinova, and V. Gudimetla, "Adaptive beam director for a tiled fiber array," in *Advanced Maui Optical and Space Surveillance Technologies Conference* (2006).
17. M. Vorontsov, T. Weyrauch, S. Lachinova, M. Gatz, and G. Carhart, "Speckle-metric-optimization-based adaptive optics for laser beam projection and coherent beam combining," Opt. Lett. **37**, 2802–2804 (2012).
18. Y. Li, J. Guo, L. Liu, T. Wang, W. Tang, and Z. Jiang, "Clipped speckle autocorrelation metric for spot size characterization of focused beam on a diffuse target," Opt. Express **23**, 7424–7441 (2015).
19. S. O. Rice, "Mathematical analysis of random noise," Bell Syst. Tech. J. **23**, 146–156 (1944).
20. R. D. Bahuguna, K. K. Gupta, and K. Singh, "Expected number of intensity level crossings in a normal speckle pattern," J. Opt. Soc. Am. **70**, 874–876 (1980).